Excited states of methylene from quantum Monte Carlo

Paul Zimmerman, Julien Toulouse, Zhiyong Zhang, Charles Musgrave, C. Umrigar

To cite this version:

Paul Zimmerman, Julien Toulouse, Zhiyong Zhang, Charles Musgrave, C. Umrigar. Excited states of methylene from quantum Monte Carlo. The Journal of Chemical Physics, 2009, 131 (12), pp.124103. 10.1063/1.3220671 . hal-03740048

Excited states of methylene from quantum Monte Carlo

Paul M. Zimmerman[1],* Julien Toulouse[2,3],† Zhiyong
Zhang[1],* Charles B. Musgrave[4],* and C. J. Umrigar[5]‡

[1] *Dept. of Chemical Engineering, Stanford University, Stanford, CA 94305, USA.*

[2] *UPMC Univ Paris 06, UMR 7616, Laboratoire de Chimie Théorique, 75005 Paris, France.*

[3] *CNRS, UMR 7616, Laboratoire de Chimie Théorique, 75005 Paris, France.*

[4] *Department of Chemical and Biological Engineering,*
University of Colorado at Boulder, Boulder, CO, 80309

[5] *Laboratory of Atomic and Solid State Physics,*
Cornell University, Ithaca, New York 14853, USA.

(Dated: August 13, 2009)

Abstract

The ground and lowest three adiabatic excited states of methylene are computed using the variational Monte Carlo (VMC) and diffusion Monte Carlo (DMC) methods using progressively larger Jastrow-Slater multideterminant complete-active-space (CAS) wave functions. The highest of these states has the same symmetry, $^1A_1$, as the first excited state. The DMC excitation energies obtained using any of the CAS wave functions are in excellent agreement with experiment, but single-determinant wave functions do not yield accurate DMC energies of the states of $^1A_1$ symmetry, indicating that it is important to include in the wave function Slater determinants that describe static (strong) correlation. Excitation energies obtained using recently proposed pseudopotentials (Burkatzki et al, JCP 126, 234105) differ from the all-electron excitation energies by at most 0.04 eV.

---

*Electronic address: `zimmerman@stanford.edu`

†Electronic address: `julien.toulouse@upmc.fr`

‡Electronic address: `CyrusUmrigar@cornell.edu`

I. INTRODUCTION

There is a considerable need for excited-state electronic-structure calculations for research on solar energy, photoelectrochemistry and catalysis, and other light-driven phenomenon. Quantum Monte Carlo (QMC) is an accurate and highly parallelizable approach for calculating the electronic structure of atoms, molecules and solids [1–3]. Although QMC has mostly been used for computing the lowest energy states of a given symmetry, methods have been developed [4–11] for computing true excited states as well.

The two most commonly used variants, variational Monte Carlo (VMC) and diffusion Monte Carlo (DMC), use a flexible trial wave function, generally consisting for atoms and molecules of a Jastrow factor multiplied by a short expansion in configuration state functions (CSFs), each consisting of a linear combination of Slater determinants of orbitals expanded in a Slater or Gaussian basis. The trial wave functions employed determine the accuracy of VMC calculations, and also of DMC calculations performed with the fixed-node approximation in which the nodes of the trial wave function are used to enforce the fermionic antisymmetry constraint. Recently, the linear optimization method has been extended, from optimizing linear parameters [5] to efficiently optimizing all the parameters [12–14] of ground-state wave functions by minimizing the VMC energy.

VMC and DMC calculations of excitation energies in molecules have been most often performed without reoptimizing the determinantal part of the wave function in QMC in the presence of the Jastrow factor (see, e.g., Refs. 15–19). Filippi and coworkers have optimized Jastrow and determinantal parameters for excited states of various molecules using the energy fluctuation potential method [6, 7, 20] and the linear optimization method [8–10], including excited states that are not the lowest ones in their irreducible representations using a general state-average strategy.

In this work, we investigate QMC calculations of excited states of methylene (CH_2). This system has served as an important benchmark for electronic-structure methods due to its small size and because some of its excited states are difficult to describe accurately [21–28]. While the ground state ($1\,^3B_2$) and second excited state ($1\,^1B_2$) [29] can be described well with a single CSF with a dominant configuration $(1a_1)^2(2a_1)^2(1b_1)^2(3a_1)(1b_2)$, the first excited state ($1\,^1A_1$) and third excited state ($2\,^1A_1$) are multiconfiguration states with considerable admixture of the configurations $(1a_1)^2(2a_1)^2(1b_1)^2(3a_1)^2$ and $(1a_1)^2(2a_1)^2(1b_1)^2(1b_2)^2$ and are therefore more challenging to calculate. To achieve accurate excitation energies, both static and dynamic correlation must be treated accurately. In general, methods such as full configuration interaction (FCI) [26], multireference configuration interaction [25], and spin-flip or multireference coupled cluster [27, 30] are all capable of describing these states, but suffer from poor scaling and the need for large basis sets and even extrapolation to the complete-basis set limit. These methods become computationally infeasible for large systems. Time-dependent density functional theory can be applied to larger systems, but chemical accuracy is not reached [31].

We apply the linear optimization method to optimize Jastrow-Slater multideterminant complete active space (CAS) wave functions for CH_2. For the ground state $1\,^3B_2$ and for the excited states $1\,^1A_1$ and $1\,^1B_2$, which are the lowest states in their irreducible representations, we minimize the energy using the standard linear optimization method. For the second excited state of $^1A_1$ symmetry, we perform a state-specific (as opposed to a state-averaged) optimization by simply targeting the second eigenvector of the Hamiltonian matrix of the linear optimization method. We study the effect of the CAS size, the effect of optimizing different types of parameters and the use of a pseudopotential on the results, and demonstrate that excitation energies can be calculated with chemical accuracy in DMC.

II. METHODOLOGY

We use Jastrow-Slater wave functions parametrized as [12, 14]

$$|\Psi(\mathbf{p})\rangle \;=\; \hat{J}(\boldsymbol{\alpha}) e^{\hat{\kappa}(\boldsymbol{\kappa})} \sum_{I=1}^{N_{\mathrm{CSF}}} c_I |C_I\rangle, \qquad (1)$$

where $\hat{J}(\boldsymbol{\alpha})$ is a Jastrow factor operator, $e^{\hat{\kappa}(\boldsymbol{\kappa})}$ is the orbital rotation operator and $|C_I\rangle$ are CSFs. Each CSF is a symmetry-adapted linear combination of Slater determinants of single particle orbitals which are expanded in basis functions. The parameters $\mathbf{p} = (\boldsymbol{\alpha}, \mathbf{c}, \boldsymbol{\kappa})$ to optimize are the Jastrow parameters $\boldsymbol{\alpha}$, the CSF coefficients $\mathbf{c}$ and the orbital rotation parameters $\boldsymbol{\kappa}$. The exponents of the basis functions are kept fixed in this work, although it is possible to optimize them [14, 32]. The Jastrow factor includes explicit electron-electron, electron-nucleus and electron-electron-nucleus correlation terms, accounting for dynamic correlation. The (short) CSF expansion accounts for static correlation.

All calculations are performed in C_{2v} symmetry using, for each state, the geometries from Sherrill *et al.* [26] which were generated using FCI with a triple-zeta, double polarization (TZ2P) basis. The initial CSF and orbital coefficients are taken from restricted Hartree-Fock (RHF) or multiconfiguration self-consistent field (MCSCF) CAS calculations using the GAMESS software package [33]. The orbital symmetries included in the CAS space are from the RHF orbital ordering in the all-electron ground state, which is a_1(core), a_1, b_1, a_1, b_2, a_1 and b_1. Since QMC calculations do not require a very large basis, we choose the polarized triple-zeta VB1 Slater basis of Ref. 34 for all-electron (AE) computations, and the pseudopotentials and the triple-zeta Gaussian basis of Ref. 35 for pseudopotential (PSP) computations. Each Slater function of the VB1 basis is actually expanded in GAMESS as a sum over 14 Gaussian basis functions. The QMC calculations are then done with the program CHAMP [36] (using the true VB1 Slater basis set rather than its Gaussian expansion).

The parameters are optimized with the linear energy minimization method [12–14], using an efficient Metropolis algorithm [37]. In this method, at each optimization step, the normalized wave function is expanded around the current parameters $\mathbf{p}^0$ to linear order in the parameter variations $\Delta\mathbf{p} = \mathbf{p} - \mathbf{p}^0$, and the energy is minimized by solving the following generalized eigenvalue equation, with the matrix elements computed using a finite VMC sample [14]

$$\begin{pmatrix} E_0 & \mathbf{g}_R^{\mathrm{T}}/2 \\ \mathbf{g}_L/2 & \overline{\mathbf{H}} \end{pmatrix} \begin{pmatrix} 1 \\ \Delta\mathbf{p} \end{pmatrix} = E \begin{pmatrix} 1 & \mathbf{0}^{\mathrm{T}} \\ \mathbf{0} & \overline{\mathbf{S}} \end{pmatrix} \begin{pmatrix} 1 \\ \Delta\mathbf{p} \end{pmatrix}, \tag{2}$$

where E_0 is the estimate of the current energy, $\mathbf{g}_L$ and $\mathbf{g}_R$ are two estimates of the energy gradient, $\overline{\mathbf{H}}$ and $\overline{\mathbf{S}}$ are estimates of the Hamiltonian and overlap matrices in the basis of the first-order derivatives of the wave function. One eigenvector $\Delta\mathbf{p}$ is then selected and used to update the parameters in the current wave function, $\mathbf{p}^0 \to \mathbf{p}^0 + \Delta\mathbf{p}$. The procedure is iterated until convergence.

For the ground state $1\,{}^3\mathrm{B}_2$ and for the excited states $1\,{}^1\mathrm{A}_1$ and $1\,{}^1\mathrm{B}_2$, which are the lowest ones in their irreducible representations, we select the eigenvector $\Delta\mathbf{p}$ corresponding to the lowest eigenvalue. For the excited state $2\,{}^1\mathrm{A}_1$ which is not the lowest one in its irreducible representation, we take the eigenvector corresponding to the second lowest eigenvalue. This corresponds to a saddle point rather than a minimum in the parameter space. The optimization of the $2\,{}^1\mathrm{A}_1$ state is less stable than for the other states. The optimization can fail in two ways: the parameters may never converge to a good approximation of an eigenstate, or root flipping can occur, i.e. the eigenvalue of the optimized $2\,{}^1\mathrm{A}_1$ state becomes lower than the eigenvalue of the unoptimized $1\,{}^1\mathrm{A}_1$ state. In this latter case, the relative sign of CSF coefficients of the two dominant configurations indicated in the Introduction can change from one optimization iteration to another. (For the $1\,{}^1\mathrm{A}_1$ state they have opposite sign, whereas for the $2\,{}^1\mathrm{A}_1$ state they have the same sign.) However, if we first optimize the nonlinear Jastrow and orbital parameters for the $1\,{}^1\mathrm{A}_1$ state (but at the geometry of the $2\,{}^1\mathrm{A}_1$ state), and use these optimized parameters as a starting point for optimizing the $2\,{}^1\mathrm{A}_1$ state, then these problems are rarely observed. Thus, one can fully optimize wave functions for each state separately. We note, however, that for systems where the orbitals obtained from optimizing the ground state are very different from those obtained from optimizing the excited state, this simple approach may fail and one may need to use a more general state-averaged approach [8–10].

Once the trial wave functions have been optimized, we perform DMC calculations, within the short-time and fixed-node (FN) approximations using an efficient DMC algorithm featuring small time-step errors [38]. For the PSP calculations, we additionally use the localization approximation [39]. The time step used for all the DMC computations is 0.01 Hartree^{-1} and the DMC energies are converged to within a statistical uncertainty of 0.1 mHartree ($\approx$ 0.003 eV) or less.

In this study we compare QMC results using RHF, CAS(2,2), CAS(4,4) and CAS(6,6) initial wave functions and optimization of the Jastrow parameters only ("Jastrow-optimized"), simultaneous optimization of the Jastrow and CSF parameters ("Jastrow-CSF-optimized") and simultaneous optimization of the Jastrow, CSF and orbital parameters ("Fully-optimized").

III. ALL-ELECTRON RESULTS

A. Convergence of total energies

Table I and Figures 1, 2, 3 and 4 show the convergence of VMC and DMC total energies for the ground state ($1\,^3\mathrm{B}_2$) and the first three excited states ($1\,^1\mathrm{A}_1$, $1\,^1\mathrm{B}_2$, $2\,^1\mathrm{A}_1$) of methylene using progressively larger CAS wave functions. In each figure, the upper three curves are the VMC energies and the lower three are DMC energies. Within each triplet of energies, the upper curve was obtained by optimizing the Jastrow parameters only, the middle curve was obtained optimizing the Jastrow and the CSF parameters and the bottom curve was obtained optimizing the Jastrow, CSF and orbital parameters. The energies in the table were obtained optimizing the Jastrow, CSF and orbital parameters. When the CSF and orbitals parameters are optimized, the energies go down monotonically with increasing CAS size, as they must. On the other hand, when only the Jastrow parameters are optimized, keeping the CSF and orbital coefficients fixed at their MCSCF values, the energies can go up with increasing CAS size, as has been previously been noted by two of the authors [13].

When Jastrow, CSF and orbital parameters are optimized, the energy goes down only slightly as the CAS size is increased. The CAS(2,2) for the $1\,^3\mathrm{B}_2$ and $1\,^1\mathrm{B}_2$ states corresponds to a single CSF and these states have single-reference character. The CAS(2,2) for the $1\,^1\mathrm{A}_1$ and $2\,^1\mathrm{A}_1$ states have two CSFs and these states have multireference character. Hence the $1\,^1\mathrm{A}_1$ shows a significant decrease in energy going from the RHF to the CAS(2,2) initial wave function, and the $2\,^1\mathrm{A}_1$ state cannot be described by Hartree Fock.

From Table I we note that despite the fact that the QMC calculations employ a smaller basis than the FCI/TZ2P calculations, not only the DMC energies but even the VMC energies are significantly lower than the FCI/TZ2P energies. This is a manifestation of the well-known fact that QMC energies are less sensitive to the basis and the number of determinants in the wave function. Since the VMC and DMC energies are upper bounds to the true energy, they are more accurate than the FCI/TZ2P energies. Also shown in Table I are energies for the lower two states from restricted coupled cluster singles doubles with perturbative triples (RCCSD(T)), contracted multireference configuration interaction (CMRCI), and CMRCI with the Davidson correction (CMRCI+Q) from Ref. 40. Each of these energies has been extrapolated to the infinite basis set limit, using energies from double to quintuple-zeta basis sets.

B. Convergence of excitation energies

Table I and Figures 5, 6 and 7 show the convergence of the first three adiabatic excitation energies of methylene as a function of the CAS size. The lower two excitation energies, $1\,^1\mathrm{A}_1$-$1\,^3\mathrm{B}_2$ and $1\,^1\mathrm{B}_2$-$1\,^3\mathrm{B}_2$, obtained from DMC using the Jastrow, CSF and orbital optimized wave functions are independent of CAS size within statistical uncertainty and in excellent agreement with the experimental (non-relativistic, Born-Oppenheimer, and corrected to remove zero-point energy) values of 0.406 eV [23] and 1.415 eV [24, 41]. In contrast the excitation energies obtained from FCI are too high by 0.076 and 0.127 eV respectively. Also shown in Table I are the MCSCF energies. The excitation energies from MCSCF change by 0.3 eV upon varying the CAS size, whereas the DMC energies vary by only 0.01 eV for the first two excitation energies and by 0.08 eV for the third excitation energy, demonstrating the robustness of the DMC method.

Although the multiconfigurational excited state $2\,^1\mathrm{A}_1$ has been theoretically hypothesized as important in reactions involving methylene, no experimental results are available and it is difficult to describe theoretically. The excitation energy obtained from DMC with the Jastrow, CSF and orbital optimized wave functions (see Table I) shows a small but statistically significant decrease with increasing CAS size. Our best estimate of this excitation energy, 2.524(4) eV, obtained with the CAS(6,6) wave function, is 0.15 eV lower that the value from FCI.

C. Test of CAS orbital choice

The symmetries of the orbitals in the CAS wave functions are chosen by picking the appropriate number of lowest energy orbitals from a Hartree-Fock calculation of the ground state. This is a simple choice that requires no chemical insight but it need not be the choice that yields the best energies. For the $1\,^1A_1$ state we tested the effect of changing the CAS(6,6) space by swapping the highest virtual orbital with an inactive orbital. (The core 1s orbitals are sufficiently low in energy that including them in the CAS space is unlikely to significantly improve the energy.) The virtual orbitals are of symmetries b_2 a_1 b_1. We exchanged the highest lying b_1 orbital with an a_1 orbital, making the virtual orbitals: b_2 a_1 a_1. The MCSCF energy using this new CAS is 0.388 eV higher than the energy from the original CAS space. However, the DMC energies, obtained using Jastrow and CSF optimized wave functions is higher by only 0.031(4) eV and that obtained using the Jastrow, CSF and orbital optimized wave function is higher by only 0.019(4) eV.

D. Test of CSF cutoff

For large systems it becomes computationally expensive to include all the determinants from CAS wave functions in the QMC calculations. Hence it is common practice to include only those CSFs that have coefficients in the MCSCF calculation larger than some threshold. In Table II we show the energies for the CAS(4,4) and CAS(6,6) wave functions using cutoffs of 0.01 and 0.05 respectively. The DMC excitation energies are still within chemical accuracy (0.04 eV) of the experimental values.

IV. TEST OF PSEUDOPOTENTIALS

For large systems, in order to keep the computational cost manageable, it becomes necessary to eliminate the core electrons using nonlocal pseudopotentials. Here we employ the excitation energies of methylene as a test of the accuracy of a recently proposed set of pseudopotentials [35] that were constructed for use in QMC calculations. Table III shows the total energies and excitation energies obtained using these pseudopotentials for carbon and hydrogen. The excitation energies obtained using these pseudopotentials show small deviations from the all-electron values (averaged over the three CAS sizes) of -0.03(1), +0.04(1) and +0.02(1) eV for the first three excited states.

V. CONCLUSIONS

We have employed VMC and DMC methods to compute the four lowest energy states of methylene using progressively larger Jastrow-Slater multideterminant CAS wave functions, the fourth state having the same symmetry as the second state. Provided that the Jastrow, CSF and orbital parameters are optimized simultaneously, the excitation energies obtained from DMC are almost independent of the CAS size. Excitation energies for the lower two excited states, obtained from even the smallest CAS wave functions, are in excellent agreement with experiment, indicating that it is sufficient to include in the wave function just those determinants that describe static correlation to obtain an accurate wave function nodal surface for the fixed-node DMC calculations. For the highest state, we make a prediction for the excitation energy since an accurate experimental value is lacking. We find that excitation energies from recently proposed pseudopotentials for carbon and hydrogen differ from the all-electron excitation energies by at most 0.04 eV.

VI. ACKNOWLEDGEMENTS

This work was supported in part by a Stanford Graduate Fellowship (PMZ), by DOE grant DE-FG02-07ER46365 and NSF grant EAR-0530813. The computations were performed using computers at the National Nanotechnology Infrastructure Network (NNIN). We thank Claudia Filippi for useful discussions.

---

[1] W. M. C. Foulkes, L. Mitas, R. J. Needs, and G. Rajagopal, Rev. Mod. Phys. **73**, 33 (2001).

[2] M. P. Nightingale and C. J. Umrigar, eds., *Quantum Monte Carlo Methods in Physics and Chemistry*, NATO ASI Ser. C 525 (Kluwer, Dordrecht, 1999).

[3] S. Zhang and H. Krakauer, Phys. Rev. Lett. **90**, 136401 (2003).

[4] D. M. Ceperley and B. Bernu, J. Chem. Phys. **89**, 6316 (1988).

[5] M. P. Nightingale and V. Melik-Alaverdian, Phys. Rev. Lett. **87**, 043401 (2001).

[6] F. Schautz and C. Filippi, J. Chem. Phys. **120**, 10931 (2004).

[7] F. Schautz, F. Buda, and C. Filippi, J. Chem. Phys. **121**, 5836 (2004).

[8] F. Cordova, L. J. Doriol, A. Ipatov, M. E. Casida, C. Filippi, and A. Vela, J. Chem. Phys. **127**, 164111 (2007).

[9] E. Tapavicza, I. Tavernelli, U. Rothlisberger, C. Filippi, and M. E. Casida, J. Chem. Phys. **129**, 124108 (2008).

[10] C. Filippi, M. Zaccheddu, and F. Buda (2009), unpublished.

[11] W. Purwanto, S. Zhang, and H. Krakauer, J. Chem. Phys. **130**, 094107 (2009).

[12] J. Toulouse and C. J. Umrigar, J. Chem. Phys. **126**, 084102 (2007).

[13] C. J. Umrigar, J. Toulouse, C. Filippi, S. Sorella, and R. G. Hennig, Phys. Rev. Lett. **98**, 110201 (2007).

[14] J. Toulouse and C. J. Umrigar, J. Chem. Phys. **128**, 174101 (2008).

[15] J. C. Grossman, M. Rohlfing, L. Mitas, and S. G. L. abd M. L. Cohen, Phys. Rev. Lett. **86**, 472 (2001).

[16] A. Aspuru-Guzik, O. E. Akramine, J. C. Grossman, and W. A. Lester, J. Chem. Phys. **120**, 3049 (2004).

[17] N. D. Drummond, A. J. Williamson, R. J. Needs, and G. Galli, Phys. Rev. Lett. **95**, 096801 (2005).

[18] M. L. Tiago, P. R. C. Kent, R. Q. Hood, and F. A. Reboredo, J. Chem. Phys. **129**, 084311 (2008).

[19] T. Bouabca, N. B. Amor, D. Maynau, and M. Caffarel, J. Chem. Phys. **130**, 114107 (2009).

[20] A. Scemama and C. Filippi, Phys. Rev. B **73**, 241101 (2006).

[21] P. J. Reynolds, M. Dupuis, and W. A. Lester, J. Chem. Phys. **82**, 1983 (1985).

[22] H. F. Schaefer, Science **231**, 1100 (1986).

[23] P. Jensen and P. R. Bunker, J. Chem. Phys. **89**, 1327 (1988).

[24] A. Alijah and G. Duxbury, Mol. Phys. **70**, 605 (1990).

[25] N. L. Doltsinis and P. J. Knowles, J. Chem. Soc., Faraday Trans. **93**, 2025 (1997).

[26] C. D. Sherrill, M. L. Leininger, T. J. V. Huis, and H. F. Schaefer, J. Chem. Phys. **108**, 1040 (1998).

[27] L. V. Slipchenko and A. I. Krylov, J. Chem. Phys. **117**, 4694 (2002).

[28] J. R. Flores and R. J. Gdanitz, J. Chem. Phys. **123**, 144316 (2005).

[29] Note that the choice of symmetry label, B_1 or B_2 depends just on whether the molecule is in the $y-z$ or the $x-z$ plane.

[30] X. Li and J. Paldus, J. Chem. Phys. **129**, 174101 (2008).

[31] M. R. Silva-Junior, M. Schreiber, S. P. A. Sauer, and W. Thiel, Chem. Phys. **129**, 104103 (2008).

[32] The basis we used is large enough that exponent optimization does not significantly change the energy or its fluctuations, but for smaller basis sets we have obtained significant improvements by optimizing the basis exponents.

[33] M. W. Schmidt, K. K. Baldridge, J. A. Boatz, S. T. Elbert, M. S. Gordon, J. H. Jensen, S. Koseki, N. Matsunaga, K. A. Nguyen, S. J. Su, et al., J. Comput. Chem. **14**, 1347 (1993).

[34] I. Ema, J. M. García de la Vega, G. Ramírez, R. López, J. F. Rico, H. Meissner and J. Paldus, J. Comput. Chem. **24**, 859 (2003).

[35] M. Burkatzki, C. Filippi, and M. Dolg, J. Chem. Phys. **126**, 234105 (2007).

[36] CHAMP, a quantum Monte Carlo program written by C. J. Umrigar, C. Filippi and J. Toulouse, URL `http://pages.physics.cornell.edu/~cyrus/champ.html`.

[37] C. J. Umrigar, Phys. Rev. Lett. **71**, 408 (1993).

[38] C. J. Umrigar, M. P. Nightingale, and K. J. Runge, J. Chem. Phys. **99**, 2865 (1993).

[39] M. M. Hurley and P. A. Christiansen, J. Chem. Phys. **86**, 1069 (1987); B. L. Hammond, P. J. Reynolds, and W. A. Lester, Jr., ibid. **87**, 1130 (1987); L. Mitas, E. L. Shirley, and D. M. Ceperley, J. Chem. Phys. **95**, 3467 (1991).

[40] D. Woon and T. Dunning, J. Chem. Phys. **103**, 4572 (1995).

[41] The experimental results of Alijah and Duxbury (1.411 eV) are corrected to remove zero-point energy by the FCI/TZ2P results of Sherrill et al (0.004 eV).

Figures

FIG. 1: (Color online) Convergence of all-electron VMC and DMC total energies for the $1\,^3\mathrm{B}_2$ ground state of methylene with increasing CAS size.

FIG. 2: (Color online) Convergence of all-electron VMC and DMC total energies for the $1\,^1\mathrm{A}_1$ excited state of methylene with increasing CAS size.

FIG. 3: (Color online) Convergence of all-electron VMC and DMC total energies for the $1\,^1\mathrm{B}_2$ excited state of methylene with increasing CAS size.

FIG. 4: (Color online) Convergence of all-electron VMC and DMC total energies for the $2\,^1\mathrm{A}_1$ excited state of methylene with increasing CAS size.

FIG. 5: (Color online) Convergence of all-electron adiabatic excitation energies from the ground state ($1\,^3B_2$) to the first excited state ($1\,^1A_1$) with increasing CAS size. The fully-optimized DMC energies show little dependence on the CAS size. Single-determinant results from an RHF initial wave function are not shown, but produce excitation energies of 0.674(8) eV and 0.616(8) eV for fully-optimized VMC and DMC, respectively.

FIG. 6: (Color online) Convergence of all-electron adiabatic excitation energies from the ground state ($1\,^3B_2$) to the second excited state ($1\,^1B_2$) compared to CAS size. The fully-optimized DMC energies show little dependence on the CAS size.

FIG. 7: (Color online) Convergence of all-electron adiabatic excitation energies from the ground state ($1\,^3B_2$) to the third excited state ($2\,^1A_1$) with increasing CAS size.

Tables

TABLE I: Comparison of the total energies (in Hartree) and adiabatic excitation energies (in eV) of the four lowest states of methylene obtained from VMC and DMC with various Jastrow-Slater CAS wave functions (this work). The statistical uncertainty is shown in parentheses. The Jastrow, CSF and orbital parameters were simultaneously optimized. The DMC excitation energies are almost independent of the CAS size. These energies are compared to those from RCCSD(T), CMRCI and CMRCI+Q, extrapolated to the infinite basis limit (from Ref. 40), and, from FCI with triple-zeta plus two polarization function basis (from Ref. 26). The excitation energies are compared also to the experimentally derived [23, 24, 41] values reported in [26].

	CAS(2,2)	CAS(4,4)	CAS(6,6)	
		$1\,^3B_2$		
MCSCF	-38.93357	-38.93402	-38.97235	
VMC	-39.1273(2)	-39.1279(2)	-39.1327(2)	
DMC	-39.1406(1)	-39.1408(1)	-39.1428(1)	
RCCSD(T) [40]				-39.1480
CMRCI [40]				-39.1419
CMRCI+Q [40]				-39.1483
FCI [26]				-39.0667
		$1\,^1A_1$		
MCSCF	-38.91628	-38.92145	-38.95490	

VMC	-39.1124(2)	-39.1126(2)	-39.1169(2)	
DMC	-39.1255(1)	-39.1257(1)	-39.1279(1)	
RCCSD(T) [40]				-39.1329
CMRCI [40]				-39.1273
CMRCI+Q [40]				-39.1340
FCI [26]				-39.0490
		$1\,^{1}\mathrm{B}_2$		
MCSCF	-38.86919	-38.876136	-38.90403	
VMC	-39.0755(2)	-39.0758(2)	-39.0790(2)	
DMC	-39.0890(1)	-39.0891(1)	-39.0908(1)	
FCI [26]				-39.0101
		$2\,^{1}\mathrm{A}_1$		
MCSCF	-38.81211	-38.82494	-38.85686	
VMC	-39.0311(2)	-39.0334(2)	-39.0389(2)	
DMC	-39.0451(1)	-39.0465(1)	-39.0501(1)	
FCI [26]				-38.9685
		$1\,^{1}\mathrm{A}_1 - 1\,^{3}\mathrm{B}_2$		
MCSCF	0.470	0.342	0.474	
VMC	0.407(8)	0.416(8)	0.430(8)	
DMC	0.412(4)	0.412(4)	0.406(4)	
RCCSD(T) [40]				0.411
CMRCI [40]				0.398
CMRCI+Q [40]				0.389
FCI [26]				0.482
Exper. [23]				0.406
		$1\,^{1}\mathrm{B}_2 - 1\,^{3}\mathrm{B}_2$		
MCSCF	1.751	1.575	1.858	
VMC	1.411(8)	1.417(8)	1.460(8)	
DMC	1.405(4)	1.408(4)	1.416(4)	
FCI [26]				1.542
Exper. [24, 41]				1.415
		$2\,^{1}\mathrm{A}_1 - 1\,^{3}\mathrm{B}_2$		
MCSCF	3.304	2.967	3.141	
VMC	2.620(8)	2.573(8)	2.550(8)	
DMC	2.600(4)	2.566(4)	2.524(4)	
FCI [26]				2.674

TABLE II: VMC and DMC total energies (in Hartree) and adiabatic excitation energies (in eV) of the lowest four states of methylene using truncated CAS expansions. The Jastrow, CSF and orbital parameters were simultaneously optimized. The total energies are only slightly higher than those obtained from the full CAS expansion.

	CAS(4,4) (0.01 CSF cutoff)	CAS(6,6) (0.05 CSF cutoff)
	$1\,^3\mathrm{B}_2$	
complete CSFs/Dets	4/4	51/65
truncated CSFs/Dets	4/4	6/11
VMC	-39.1279(2)	-39.1302(2)
DMC	-39.1408(1)	-39.1418(1)
	$1\,^1\mathrm{A}_1$	
complete CSFs/Dets	8/10	56/104
truncated CSFs/Dets	6/7	6/13
VMC	-39.1126(2)	-39.1131(2)
DMC	-39.1256(1)	-39.1254(1)
	$1\,^1\mathrm{B}_2$	
complete CSFs/Dets	4/8	39/104
truncated CSFs/Dets	3/6	4/18
VMC	-39.0762(2)	-39.0778(2)
DMC	-39.0892(1)	-39.0900(1)
	$2\,^1\mathrm{A}_1$	
complete CSFs/Dets	8/10	56/104
truncated CSFs/Dets	7/8	4/7
VMC	-39.0333(2)	-39.0348(2)
DMC	-39.0466(1)	-39.0482(1)
	$1\,^1\mathrm{A}_1{-}^31\,\mathrm{B}_2$	
VMC	0.417(8)	0.466(8)
DMC	0.413(4)	0.444(4)
	$1\,^1\mathrm{B}_2{-}^31\,\mathrm{B}_2$	
VMC	1.408(8)	1.425(8)
DMC	1.403(4)	1.407(4)
	$2\,^1\mathrm{A}_1{-}^31\,\mathrm{B}_2$	
VMC	2.574(8)	2.596(8)
DMC	2.562(4)	2.545(4)

TABLE III: Comparison of the total energies (in Hartree) and adiabatic excitation energies (in eV), using BFD pseudopotentials [35], of the four lowest states of methylene obtained from VMC and DMC with various Jastrow-Slater CAS wave functions. The Jastrow, CSF and orbital parameters were simultaneously optimized. The VMC and DMC excitation energies are in good agreement with the all-electron and the experimental excitation energies in Table I.

	CAS(2,2)	CAS(4,4)	CAS(6,6)
		$1\,^3B_2$	
MCSCF	-6.5760	-6.5823	-6.6157
VMC	-6.7212(2)	-6.7217(2)	-6.7251(2)
DMC	-6.7289(1)	-6.7289(1)	-6.7308(1)
		$1\,^1A_1$	
MCSCF	-6.5591	-6.5643	-6.5985
VMC	-6.7070(2)	-6.7085(2)	-6.7105(2)
DMC	-6.7147(1)	-6.7156(1)	-6.7165(1)
		$1\,^1B_2$	
MCSCF	-6.5122	-6.5192	-6.5480
VMC	-6.6688(2)	-6.6689(2)	-6.6708(2)
DMC	-6.6763(1)	-6.6763(1)	-6.6773(1)
		$2\,^1A_1$	
MCSCF	-6.4539	-6.4667	-6.5000
VMC	-6.6235(2)	-6.6262(2)	-6.6301(2)
DMC	-6.6325(1)	-6.6341(1)	-6.6369(1)
		$1\,^1A_1 - 1\,^3B_2$	
MCSCF	0.461	0.489	0.469
VMC	0.386(8)	0.361(8)	0.396(8)
DMC	0.385(4)	0.362(4)	0.388(4)
		$1\,^1B_2 - 1\,^3B_2$	
MCSCF	1.905	1.715	1.842
VMC	1.425(8)	1.437(8)	1.478(8)
DMC	1.430(4)	1.430(4)	1.455(4)
		$2\,^1A_1 - 1\,^3B_2$	
MCSCF	3.322	3.142	3.147
VMC	2.656(8)	2.600(8)	2.585(8)
DMC	2.623(4)	2.580(4)	2.552(4)

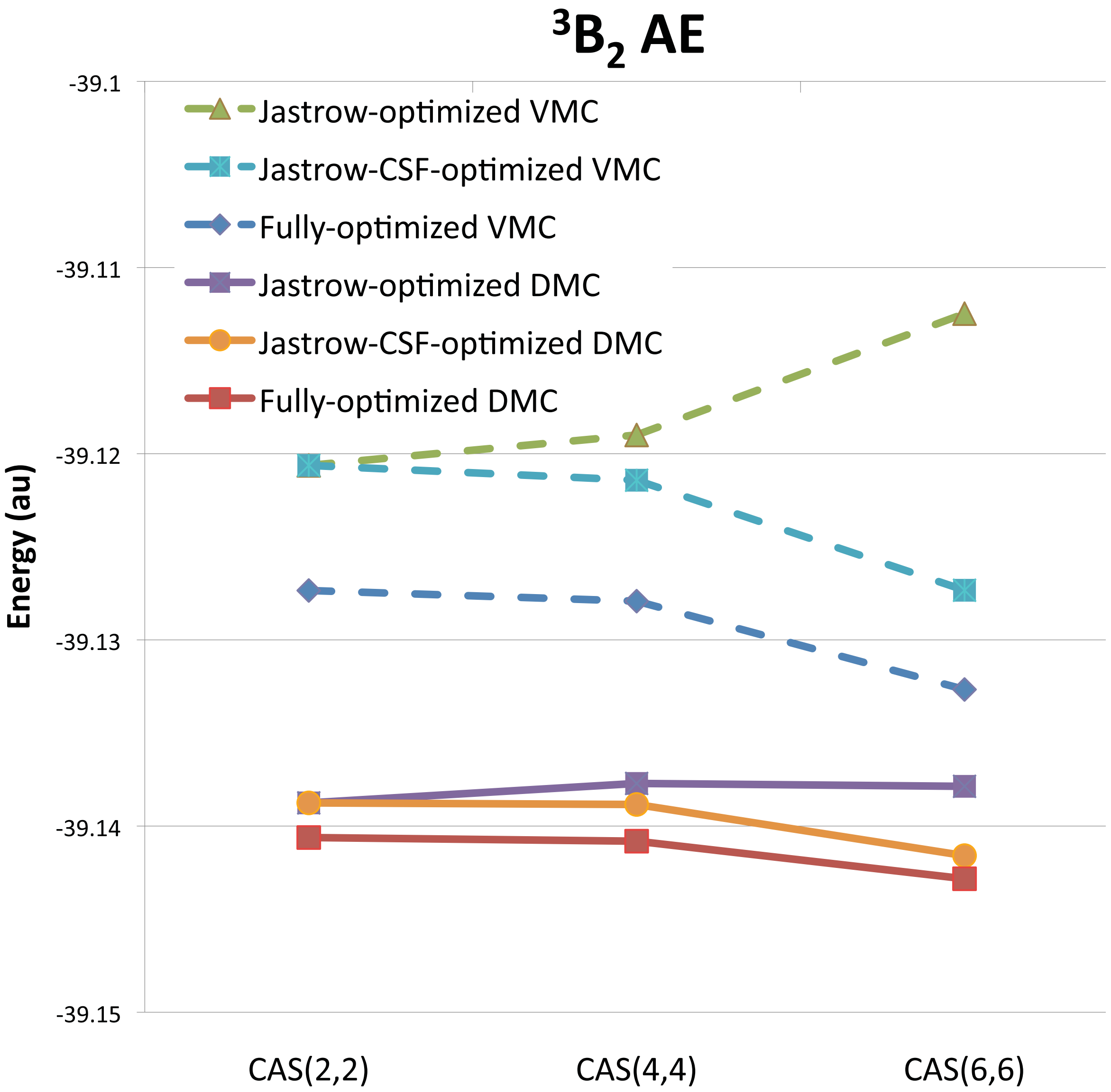
$^3B_2$ AE
Energy (au)
-39.1
-39.11
-39.12
-39.13
-39.14
-39.15
Jastrow-optimized VMC
Jastrow-CSF-optimized VMC
Fully-optimized VMC
Jastrow-optimized DMC
Jastrow-CSF-optimized DMC
Fully-optimized DMC
CAS(2,2)
CAS(4,4)
CAS(6,6)

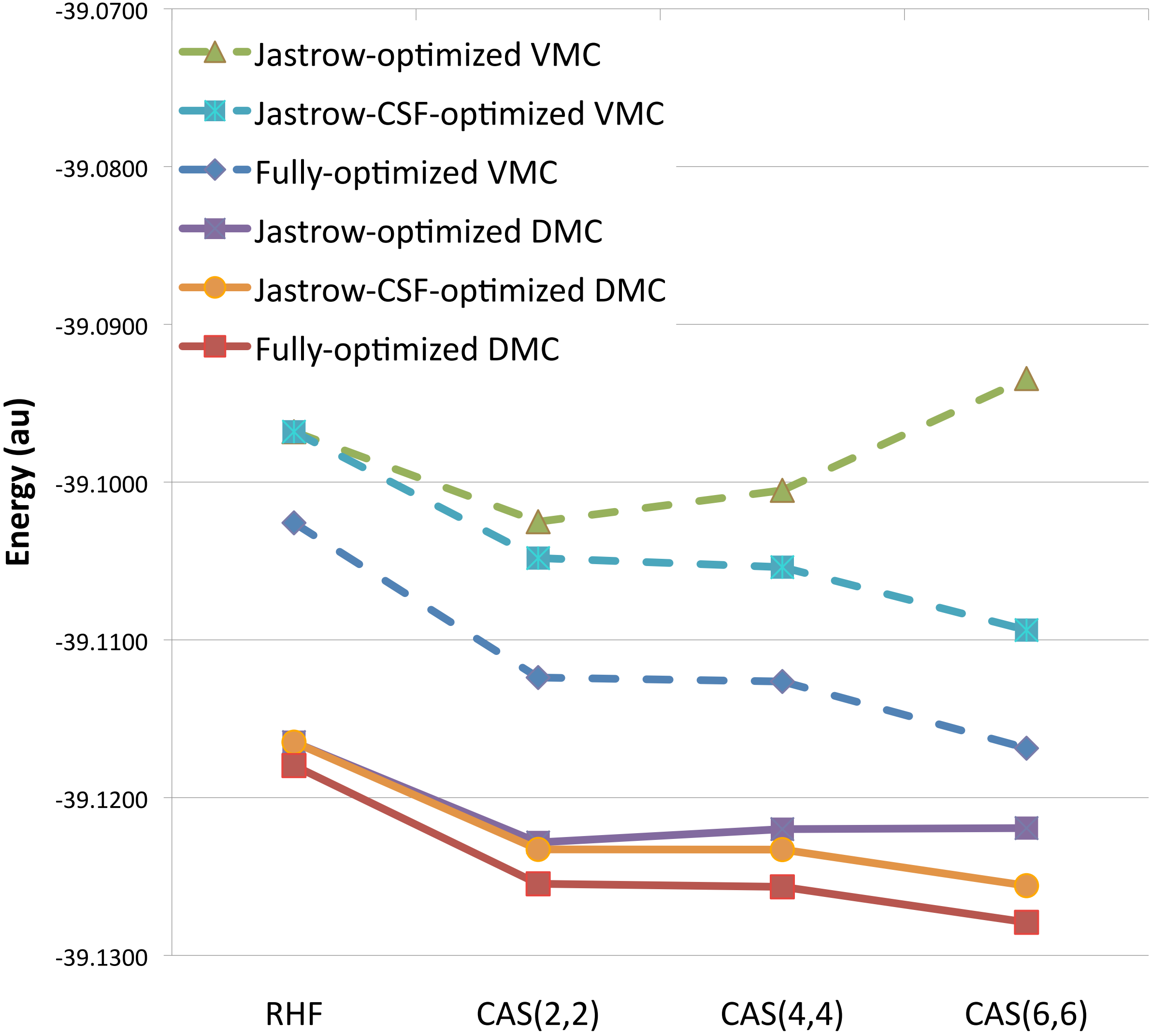

$^1A_1$ AE

Jastrow-optimized VMC
Jastrow-CSF-optimized VMC
Fully-optimized VMC
Jastrow-optimized DMC
Jastrow-CSF-optimized DMC
Fully-optimized DMC
Energy (au)
-39.0700
-39.0800
-39.0900
-39.1000
-39.1100
-39.1200
-39.1300
RHF
CAS(2,2)
CAS(4,4)
CAS(6,6)

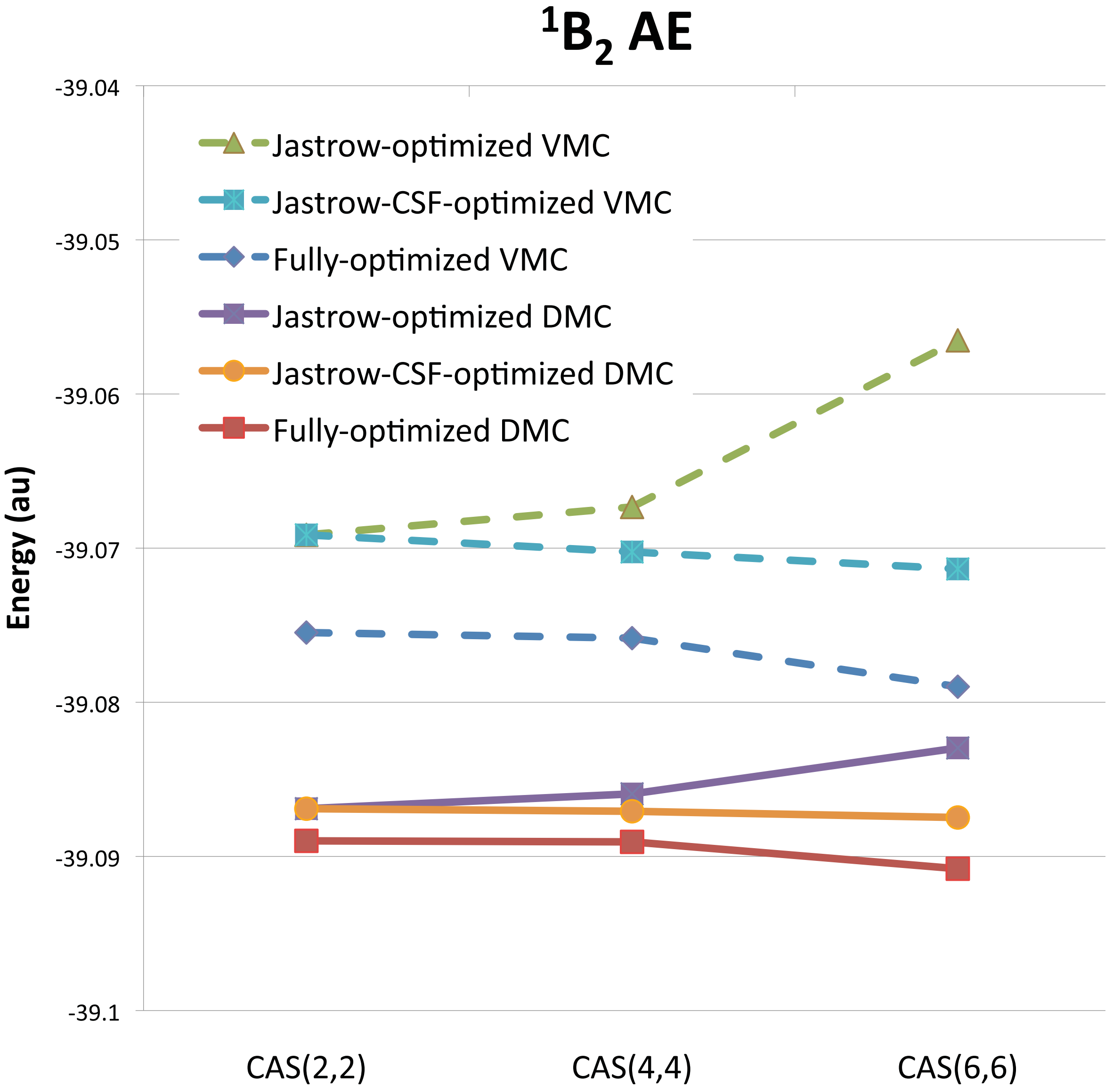

$^1B_2$ AE
-39.04
-39.05
-39.06
-39.07
-39.08
-39.09
-39.1
Energy (au)
Jastrow-optimized VMC
Jastrow-CSF-optimized VMC
Fully-optimized VMC
Jastrow-optimized DMC
Jastrow-CSF-optimized DMC
Fully-optimized DMC
CAS(2,2)
CAS(4,4)
CAS(6,6)

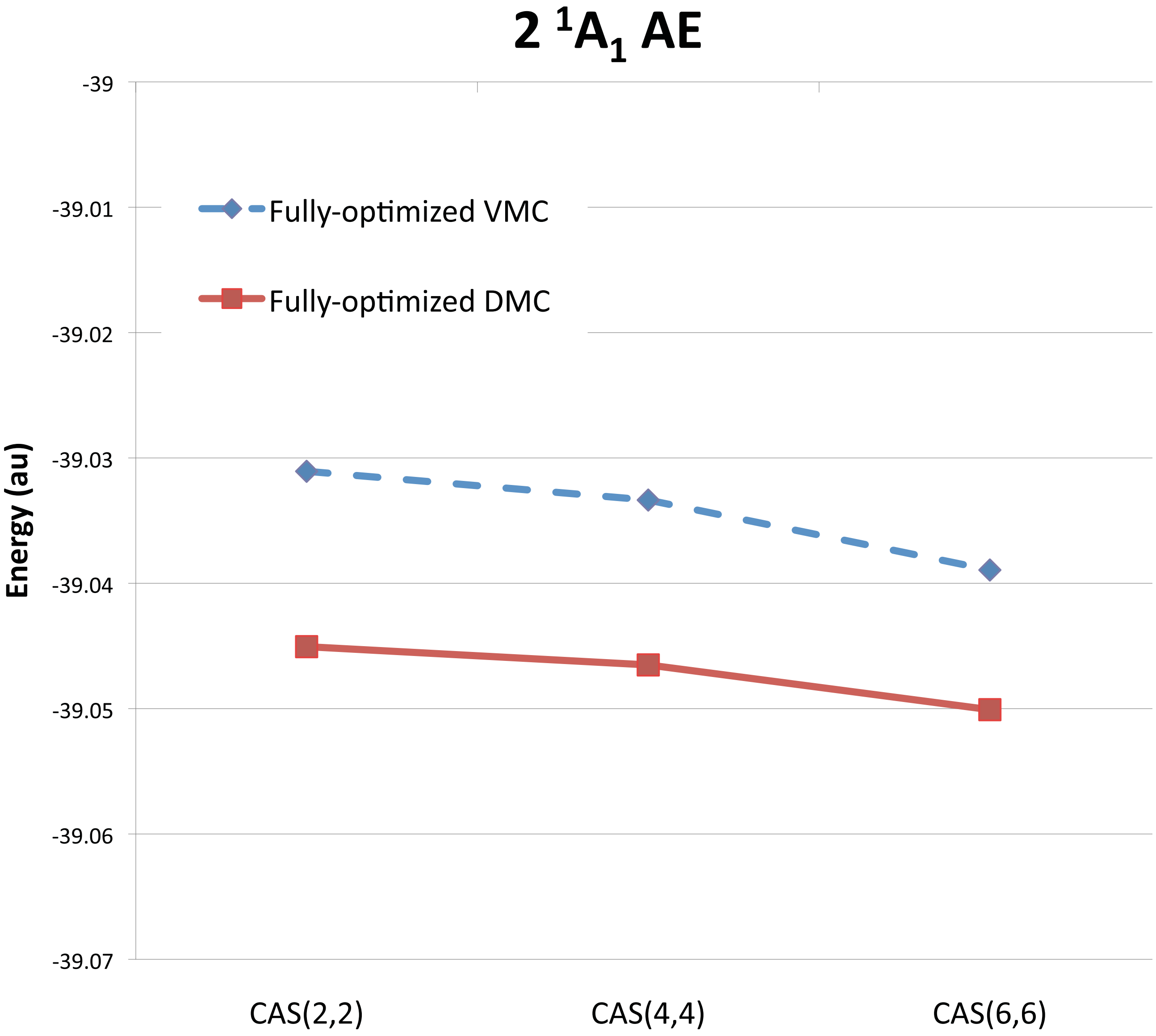
2 $^1A_1$ AE
Energy (au)
-39
-39.01
-39.02
-39.03
-39.04
-39.05
-39.06
-39.07
Fully-optimized VMC
Fully-optimized DMC
CAS(2,2)
CAS(4,4)
CAS(6,6)

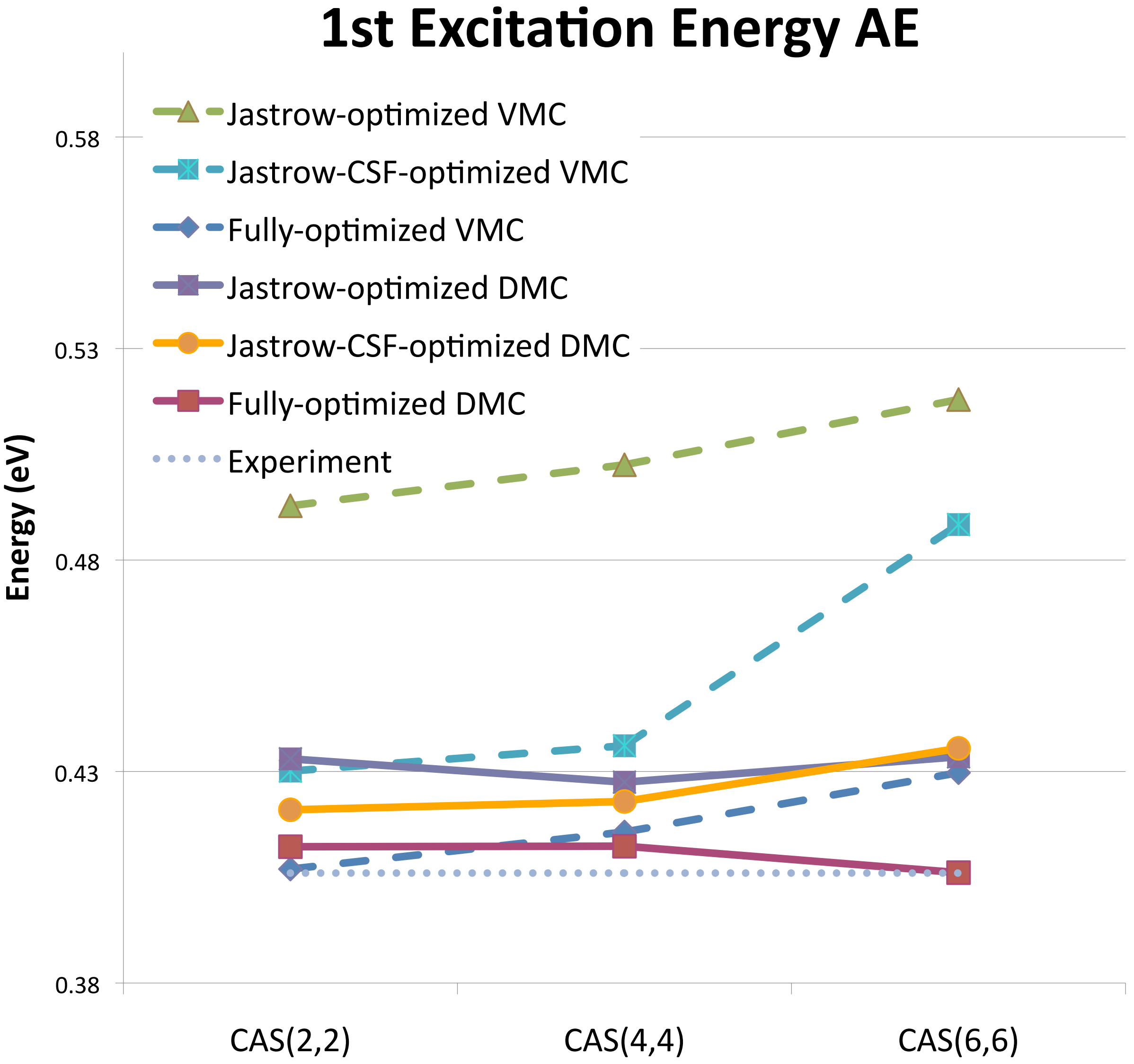
1st Excitation Energy AE
Jastrow-optimized VMC
Jastrow-CSF-optimized VMC
Fully-optimized VMC
Jastrow-optimized DMC
Jastrow-CSF-optimized DMC
Fully-optimized DMC
Experiment
Energy (eV)
0.58
0.53
0.48
0.43
0.38
CAS(2,2)
CAS(4,4)
CAS(6,6)

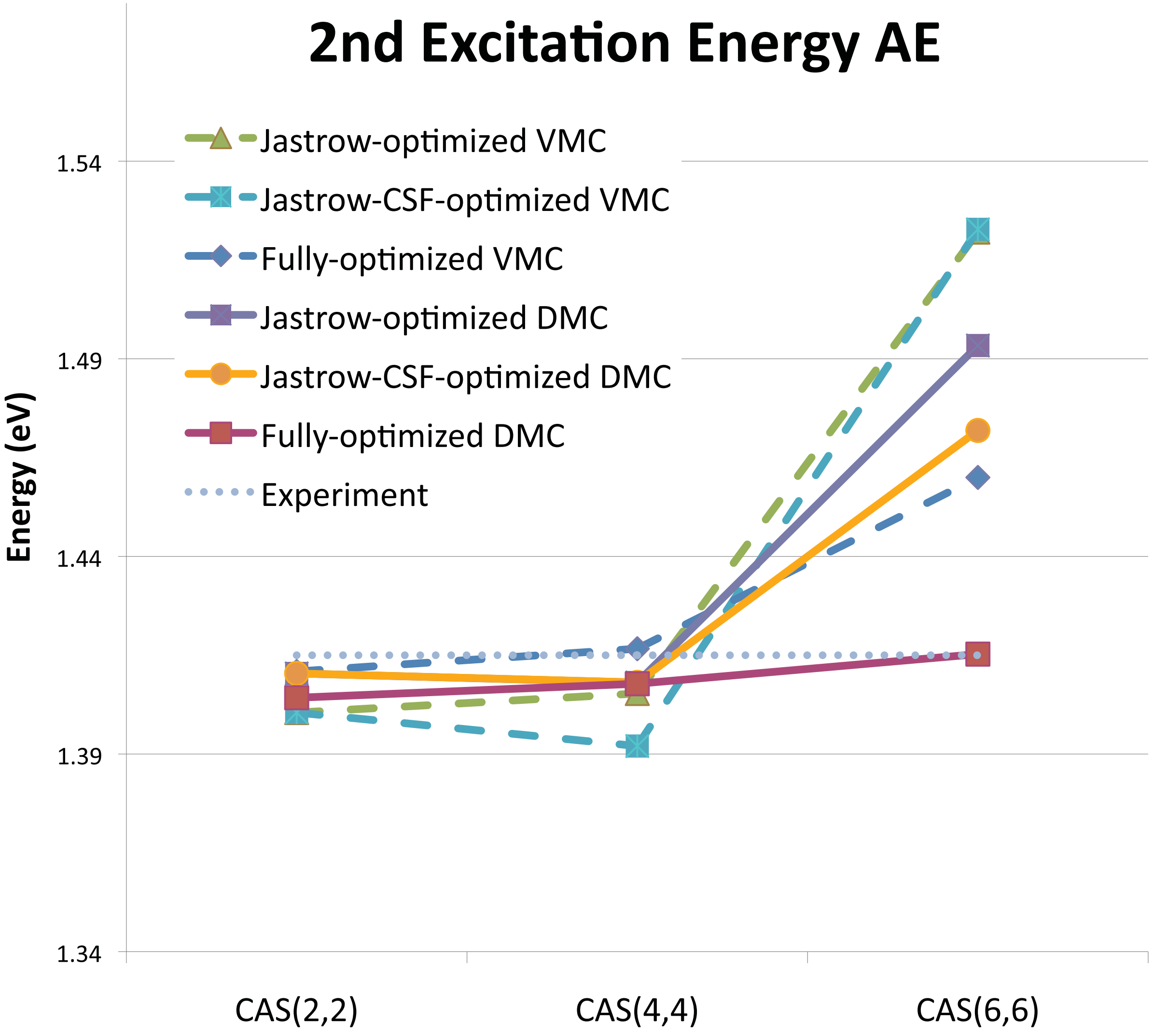
2nd Excitation Energy AE
Jastrow-optimized VMC
Jastrow-CSF-optimized VMC
Fully-optimized VMC
Jastrow-optimized DMC
Jastrow-CSF-optimized DMC
Fully-optimized DMC
Experiment
Energy (eV)
1.54
1.49
1.44
1.39
1.34
CAS(2,2)
CAS(4,4)
CAS(6,6)

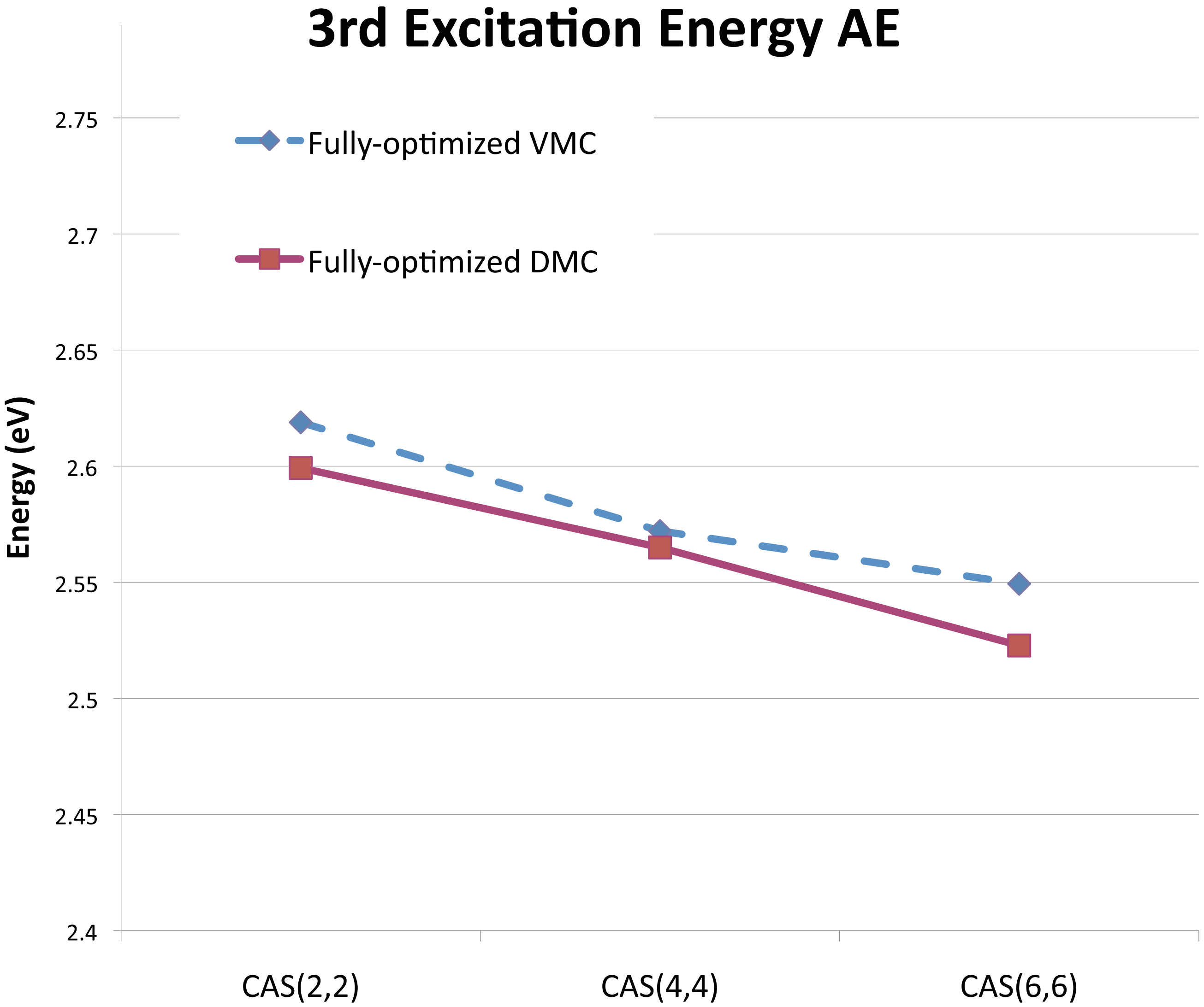
3rd Excitation Energy AE
Fully-optimized VMC
Fully-optimized DMC
Energy (eV)
2.75
2.7
2.65
2.6
2.55
2.5
2.45
2.4
CAS(2,2)
CAS(4,4)
CAS(6,6)